# Saturation effects in dynamic electrowetting

K.-L. Wang and T. B. Jones[a)]
*Department of Electrical and Computer Engineering, University of Rochester, Rochester, New York 14627*

(Received 18 October 2004; accepted 7 December 2004; published online 27 January 2005)

The same mechanism responsible for contact angle saturation of electrically stressed aqueous droplets also clamps the electromechanical force exerted on aqueous liquids in structures using dielectric-coated electrodes. Alternating current frequency strongly influences the upper limit imposed on this force. Furthermore, studies of transient, field-induced motion suggest that this mechanism is suppressed when the contact line moves rapidly along the coated electrodes. © *2005 American Institute of Physics*. [DOI: 10.1063/1.1861501]

In 1895, Pellat demonstrated the ponderomotive force exerted on dielectric media by measuring the static height-of-rise of insulating liquid between bare, metallic, parallel electrodes mounted vertically and dipped into a pool of the liquid.[1] Coating the electrodes with a thin dielectric layer and reducing the spacing to ~1 mm avoids electrolysis and excessive Joule heating, making it possible to measure the electromechanical force on aqueous media. See Fig. 1. Welters and Fokkink used this apparatus with fluorocarbon-coated electrodes to study the resulting hydrostatic equilibria,[2] discovering that the liquid column obeys the predicted square law dependence on voltage up to a threshold beyond which the liquid rises little further. Finding that this threshold corresponds to the contact angle saturation voltage, as measured independently on sessile droplets, they concluded that a single mechanism is responsible for both limits.

No general consensus exists about the mechanism that causes contact angle saturation.[3] One experimentally supported hypothesis is that, above some voltage threshold, the interface near the contact line is disrupted by the strong electric field leading to ejection of droplets and/or ions.[4,5] Another hypothesis with experimental support is that charge is injected into the dielectric layer.[6,7] This mechanism shows strong material dependence.[8] Even below the saturation threshold, there is dispute about the liquid profile near the contact line.[9,10] Whatever its origin, voltage-dependent saturation constrains the useable electromechanical force and hinders practical exploitation of electrowetting.

We report dynamic height-of-rise measurements with the apparatus of Fig. 1 indicating that the velocity of the contact line influences the onset of saturation. There are interesting implications for such a result. The success of electrowetting-based electronic paper displays[11] and voltage-controlled optoelectronic devices[12,13] depends on relatively high operational speed. Therefore, better understanding of how saturation influences the microhydrodynamics and how rapid contact line motion might defer the onset of saturation takes on real significance.

Wang and Jones used the modified Pellat experiment to investigate the frequency-dependent electromechanical force, proving that the low- and high-frequency limits correspond to electrowetting on dielectric (EWOD) and dielectrophoretic (DEP) limits, respectively. Figure 2 plots typical, static height-of-rise data versus $V_{\mathrm{rms}}^2$. The straight line predictions are based on a Maxwell stress tensor force calculation over the control volume $\Sigma$ in Fig. 1,[14]

$$h_0 = K^*(\omega) V_{\mathrm{rms}}^2,$$

where

$$K^* = \frac{\varepsilon_0 \kappa_d^2 [\varepsilon_0^2 \omega^2 (\kappa_1 - 1)(\kappa_1 d + \kappa_d D/2) + \sigma_1^2 d]}{4\rho_1 g (2d + \kappa_d D)[\varepsilon_0^2 \omega^2 (\kappa_1 d + \kappa_d D/2)^2 + \sigma_1^2 d^2]}. \quad (1)$$

Here, $\omega$=radian frequency, $d$ and $\kappa_d$=thickness and dielectric constant of the electrode coating, $\kappa_1$, $\sigma_1$, and $\rho_1$=liquid dielectric constant, electrical conductivity, and density, respectively, $\epsilon_0 = 8.854 \times 10^{-12}$ F/m, and g=9.81 m/s$^2$. With no fitting parameters, Eq. (1) closely matches data up to a threshold, above which $h_0$ deviates from predicted behavior. As frequency is increased, the transition from EWOD to DEP is apparent, i.e., $K^*$ decreases. At the same time, the maximum attainable height-of-rise actually increases because saturation is put off to a higher voltage. The electrical conductivity of the liquid may play a role here.[15,16]

When voltage is suddenly applied to the electrodes, the motion of the rising liquid column and the evolution of the meniscus can be captured with a video camera (see EPAPS Ref. 17). Figures 3(a) and 3(b), showing transient height-of-rise data culled from these videos, reveal an abrupt deceleration of the column as it nears static equilibrium. The transi-

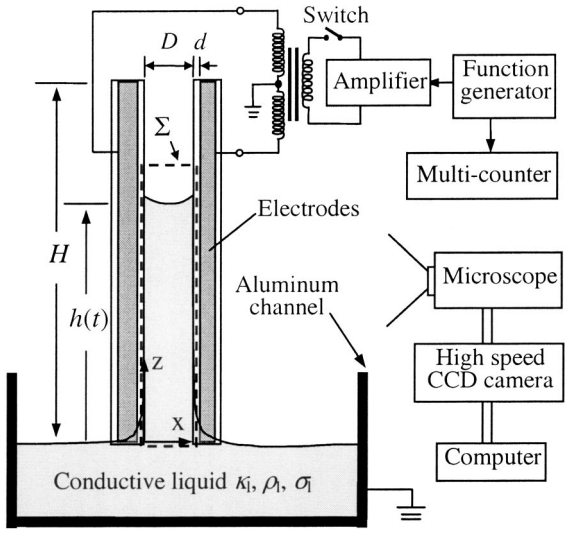


FIG. 1. The modified Pellat apparatus uses dielectric-coated, parallel electrodes to measure the electromechanical force on aqueous liquids.

a)Electronic mail: jones@ece.rochester.edu

 

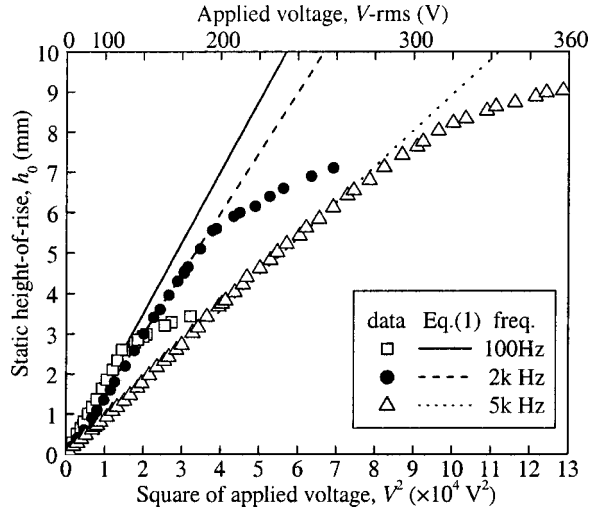


FIG. 2. Static height-of-rise data and predictive theory from Eq. (1) vs voltage squared for DI water at 100 Hz, 2 kHz, and 5 kHz: dielectric: $d = 3.5(\pm 0.5)$ $\mu$m of Parylene™, which was wiped with oil (Midel 7131) before each experiment; electrode spacing: $D = 1.0(\pm 0.05)$ mm.

tion, only evident if the applied voltage exceeds the saturation threshold, is observed for liquids ranging from deionized (DI) water to ethylene glycol, which is about 20 times more viscous. A possible explanation for such abrupt deceleration is a sudden onset in time of the contact angle saturation mechanism after the contact line has slowed down.

A reduced-order model for the transient dynamics may be formulated by imposing momentum conservation upon the rising liquid column contained in the control volume $\Sigma$ of Fig. 1. We assume $h_0 \gg W \gg D \gg d$ and that $\omega^{-1}$ is less than the characteristic mechanical time,

$$\frac{d}{dt}\left(h\frac{dh}{dt}\right) + \frac{12\mu_1}{\rho_1 D^2}\left(h\frac{dh}{dt}\right) + \frac{2\xi}{\rho_1 D}\left(\frac{dh}{dt}\right) + gh = gK(\omega)V^2u(t), \tag{2}$$

where $\mu_1$ = dynamic viscosity; $\xi$ = coefficient of dynamic contact line resistance, and $u(t)$ = unit step function. Terms on the left-hand side of Eq. (2) represent momentum, viscous drag predicated on a two-dimensional parabolic (Poiseuille) flow model,[18,19] dynamic contact line resistance attributed to molecular kinetics,[20] and gravity, respectively. The right-hand side is the electromechanical driving force. If momentum is ignored and the electromechanical driving force is replaced by a capillary term, Eq. (2) reduces to Washburn's equation for transient, capillary-driven flow.[18]

To justify using a Poiseuille velocity profile for viscous drag, the viscous diffusion time, $\tau_{vd} = \rho_1 D^2/\mu_1$, must be shorter than the mechanical response time of the column. This condition is fully met for ethylene glycol and marginally so for water. Also, the length scale for entrance effects, $L_{entry} \approx 0.06\,\mathrm{Re}\,D$, where Re = Reynolds number, must be short compared to $h(t)$. For these transient flows, $\mathrm{Re} < 10$, so the Poiseuille approximation is appropriate if $D \leqslant 1$ mm and if the voltage is high enough so that $h_0 \gg D$.

Another factor moderating concern about the Poiseuille flow assumption is that viscous drag is probably overwhelmed by contact line resistance. Decamps and De Coninck employed the contact line force to model transient electrowetting of sessile, conductive liquid droplets.[21] Following their approach, we treat $\xi$ as an adjustable parameter and use

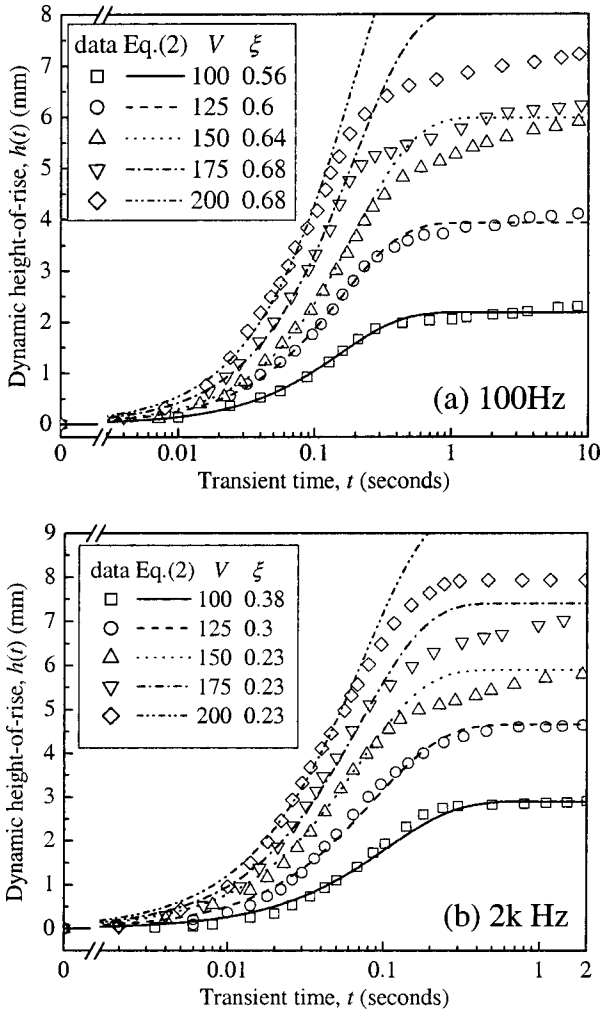


FIG. 3. Transient height-of-rise data vs time and best-fit curves from solutions to Eq. (2) for DI water at several voltages: dielectric: $d = 3.5(\pm 0.5)$ $\mu$m of Parylene™ with Midel 7131 oil film; electrode spacing: $D = 0.75(\pm 0.05)$ mm. Units of $\xi$ are N s/m$^2$. (a) 100 Hz; (b) 2 kHz.

least-squares regression to fit MATLAB™ solutions of Eq. (2) to transient data sets. Figures 3(a) and 3(b) display typical best-fit curves for each data set. For $V_{rms} \leqslant 125$ V-rms, the match is good throughout the entire transient. On the other hand, at higher voltages where abrupt deceleration occurs, a good fit is achieved only if data points after the abrupt deceleration are ignored. For consistency, curve fitting was performed repeatedly, adding one data point at a time until the fit started to deteriorate, as detected by an increase in the average mean squared error. The data keys in Figs. 3(a) and 3(b) reveal that the best-fit values for $\xi$ are reasonably constant with respect to voltage, as expected given the molecular kinetic origin of contact line resistance.[20] On the other hand, an apparent frequency dependence for $\xi$ ($\approx 0.63$ N s/m$^2$ at 100 Hz and $\sim 0.27$ N s/m$^2$ at 5 kHz) has no clear explanation, though it may be related to parametrically driven surface vibrations observed below 200 Hz. In any case, transient data over a wide range of liquid viscosities, frequencies, and voltages exhibit consistent tendencies.

Least-squares regression analyses using $\xi$ as an adjustable parameter yield far better data fits than when *added mass* or *added viscous resistance* terms are employed to account for entry effects.[19] Because the form of the contact line resistance term is so markedly different from the laminar/

viscous term in Eq. (2), $dh/dt$ versus $hdh/dt$, respectively, we conclude that the former probably dominates over the latter as the principal flow resistance mechanism. This outcome may be a consequence of charge trapping in the Parylene™. For high-speed, microfluidic actuation exploiting EWOD or DEP, these two flow resistance effects scale very differently with respect to channel length and width. Finally, there might be significant practical implications if contact angle saturation can be circumvented or deferred by rapid motion of the contact line along coated electrodes.

NIH, NSF, the Center for Future Health (University of Rochester), and the Infotonics Technology Center, Inc., supported this research.

[1]H. Pellat, C. R. Seances Acad. Sci. Paris **119**, 691 (1895).
[2]W. J. J. Welters and L. G. J. Fokkink, Langmuir **14**, 1535 (1998).
[3]M. Vallet, B. Berge, and L. Vovelle, Polymer **37**, 2465 (1996).
[4]M. Vallet, M. Vallade, and B. Berge, Eur. Phys. J. B **37**, 583 (1999).
[5]F. Mugele and S. Herminghaus, Appl. Phys. Lett. **81**, 2303 (2002).
[6]H. J. J. Verheijen and M. W. J. Prins, Langmuir **15**, 6616 (1999).
[7]B. Janocha, H. Bauser, C. Oehr, H. Brunner, and W. Göpel, Langmuir **16**, 3349 (2000).
[8]E. Seyrat and R. A. Hayes, J. Appl. Phys. **90**, 1383 (2001).
[9]K. H. Kang, Langmuir **18**, 10318 (2002).
[10]J. Buehle, S. Herminghaus, and F. Mugele, Phys. Rev. Lett. **91**, 086101 (2003).
[11]R. A. Hayes and B. J. Feenstra, Nature (London) **425**, 383 (2003).
[12]T. Krupenkin, S. Yang, and P. Mach, Appl. Phys. Lett. **82**, 316 (2003).
[13]F. Cattaneo, K. Baldwin, S. Yang, T. Krupenkin, S. Ramachandran, and J. A. Rodgers, J. Microelectromech. Syst. **12**, 907 (2003).
[14]T. B. Jones, K. L. Wang, and D. J. Yao, Langmuir **20**, 2813 (2004).
[15]B. Shapiro, H. Moon, R. L. Garrell, and C.-J. Kim, J. Appl. Phys. **93**, 5794 (2003).
[16]B. Techaumnat, S. Hamada, and T. Takuma, J. Electrost. **56**, 67 (2002).
[17]See EPAPS Document No. E-APPLAB-86-038506 for videos showing the transient behavior of the meniscus. A direct link to this document may be found in the online article's HTML reference section. The document may also be reached via the EPAPS homepage (http://www.aip.org/pubservs/epaps.html) or from ftp.aip.org in the directory /epaps/. See the EPAPS homepage for more information.
[18]E. W. Washburn, Phys. Rev. **17**, 273 (1921).
[19]W. Huang, R. S. Bhullar, and Y. C. Fung, J. Biomech. Eng. **123**, 446 (2001).
[20]T. D. Blake and J. M. Haynes, J. Colloid Interface Sci. **30**, 421 (1969).
[21]C. Decamps and J. De Coninck, Langmuir **16**, 10150 (2000).